XCFD4NRS

Experiments and CFD Codes Application to Nuclear Reactor Safety

OECD/NEA & International Atomic Energy Agency (IAEA) Workshop

Organised in Grenoble, France
10-12 September 2008

DATA OBTAINED AT HIGH COOLANT PARAMETERS SUITABLE FOR VALIDATION OF 3D-MODELS

B.A. Gabaraev, E.K. Karasyov, O.Yu. Novoselsky
(NIKIET, Moscow, Russia)

S.Z. Lutovinov, L.K. Tikhonenko, Ye.I. Trubkin
(ENIC, Elektrogorsk, Russia)

A.V. Shishov *(OKB GIDROPRESS, Podolsk, Russia)*

Abstract

Three-dimensional thermal-hydraulic models based on CFD methods are made adequate to the real conditions by selection of appropriate physical models, nodalisation and numerical techniques as well as by comparison with experimental data directly related to the phenomenon/process under investigation. Such experimental data are, e.g., the global characteristics of a device in question (circulation circuit component) or the local and global characteristics of a close analogue. For some components of the circulation circuit (more than 60 specimens) experimental data were obtained on flashing of subcooled and saturated water as well as on critical flow at pressures up to 9.3 MPa. The global characteristics found for each of the tested specimens included: pressure difference and flow rates under single-phase conditions, and critical flow rates as a function of inlet subcooling and pressure. Besides, the distribution of static pressure along the flow passage under single-phase and critical flow conditions and the void fraction at two sections along the passage were determined for the relatively long specimens. Altogether, the experimental data covered more than 5000 flow regimes of subcooled and flashing water as well as of mixed steam and water. No heat was supplied and steam was generated only due to pressure decrease in the subcooled water flow.

1. INRODUCTION

Like any other mathematical model of a process or phenomenon, CFD-based 3D-model of flow in some component needs validation / verification and subsequent adjustment with regard to the results obtained.

Two aspects are of importance in validation/verification: it is necessary to confirm, first, the adequacy of modeling the typical thermal-hydraulic processes essential to generic safety analysis and, second, the adequacy of the 3D-model describing the object of investigation. The first objective is attained by special studies with sophisticated measurement systems, which are normally conducted at rather low coolant parameters. Restriction of the parameters depends on the measurement techniques in use, [Graf, 2007]. The results are then extrapolated to high coolant temperatures and pressures. This fact together with the user effect are the reasons why the 3D-model has to be verified at some analogue whose global thermal-hydraulic parameters are known already. Agreement of the modeling results with the global parameters of the analogue will provide sufficient confidence in adequate description of the object by the 3D-model.

Most of the previous experimental studies were not intended for validation of complex thermal-hydraulic codes and are not classed with the "CFD grade experiments". This is particularly true in regard to experiments at high coolant parameters, where measurement of local characteristics is highly difficult or simply impossible. However, the global and some local parameters of high-energy coolant may serve as a good basis for validating 3D-models of single- and two-phase flows.

2. GENERAL DESCRIPTION OF EXPERIMENTAL DATA

2.1 Key phenomena

Choking of subcooled water flow, i.e. development of a critical flow, is caused by steam phase occurrence in the flow with the associated sharp decrease of sonic velocity in the two-phase mixture. Subcooled liquid in the flow boils up due to local drop of pressure below the saturation level. In other words, this may be regarded as cavitation arising on the surface of a solid body [Knapp, 1970]. Fig. 1 provides schematic explanation of the cavitation – flashing of subcooled water on a solid surface under conditions of flow acceleration.

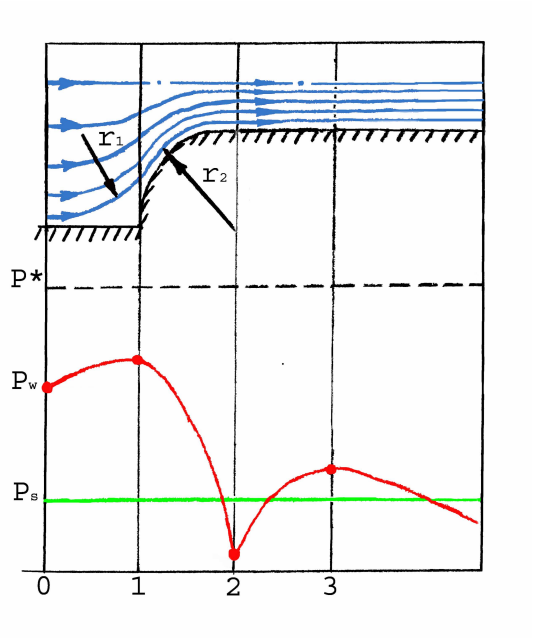

Fig. 1 Cavitation development:
P* - full pressure, P_w – static pressure on the wall, P_S – saturation pressure

Curvilinear liquid motion is accompanied by the action of centrifugal acceleration and, hence, of a centrifugal force at each point of the flow. This force is directly proportional to the squared linear (tangential) flow velocity at the given point and is in inverse proportion to the radius of the liquid particle path curvature. The force acts in the direction of the radius vector, i.e. radius of curvature. As a result, in the region between positions 0 and 1 (Fig. 1), the centrifugal force adds to the static pressure on the wall P_w, acting in the direction of radius-vector r_1 and pressing the flow against the solid surface. Within region 1-2, where the flow passes over a toroidal surface with the flow section area reduced, the centrifugal force acting in the direction of the radius-vector r_2, reduces the liquid pressure on the wall. Its maximum impact occurs at position 2, where the tangential velocity – liquid velocity at the laminar sublayer boundary – is greatest. Starting with a certain value of the liquid velocity, the centrifugal force becomes strong enough to compensate the difference between the existing static pressure on the wall, P_w, and the saturation pressure, P_s, at the current flow temperature. Subsequent increase of this difference will lead to development of steam nuclei on the washed surface and to generation of cavitation bubbles in the flow.

Clearly, two-phase versions of 3D hydrodynamic codes should allow simulating this phenomenon. The adequacy of such models may be checked against the results of studies described below.

2.2 Experimental facility

Experiments with various hydraulic devices – small- and full-size models of circulation circuit components – were staged at a facility where a special coolant treatment system, comprising a steam-water mixer and control valves, delivered fluid of strictly set parameters to the inlet of tested specimens. Fig. 2 is a general view of the test section with a specimen inside it, i.e. a tube with a sharp inlet edge. Two pairs of flanged branches were provided to accommodate γ-ray devices. As may be seen, measurement of fluid density (void fraction) was only possible with sufficiently long specimens. The γ-ray device configuration is shown in Fig. 3. Used as a source of γ-quanta was ^{170}Tu .

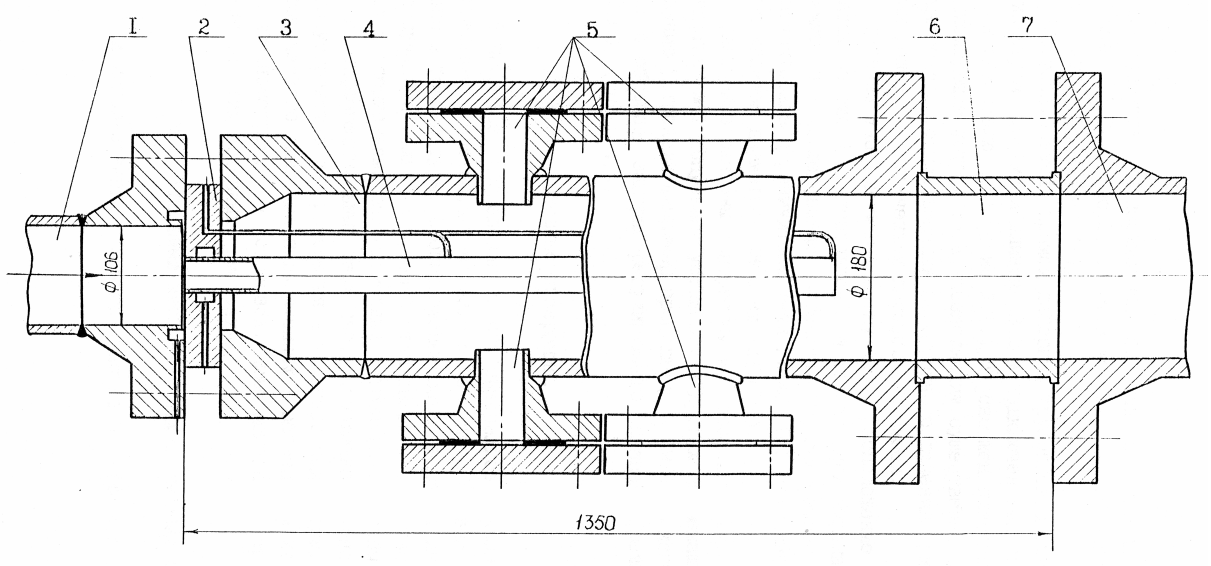

Fig. 2 Work area with a straight tube
1- pipeline from the coolant treatment system; 2 – pulse line exits;
3 – work area housing; 4 – tested channel; 5 – locations of γ-ray devices; 6 – extension; 7 – outlet pipeline.

The experimental facility allowed varying the parameters of the fluid fed to the test section within the following ranges:

- pressure, 0.15÷9.3 MPa;
- water temperature, 104÷305 ^{o}C;
- steam quality, 0÷1,0;
- steam temperature, 110÷400 ^{o}C;
- fluid flow rate, up to 23 kg/s.

The outlet pressure varied from 0.08 to 9.3 MPa.

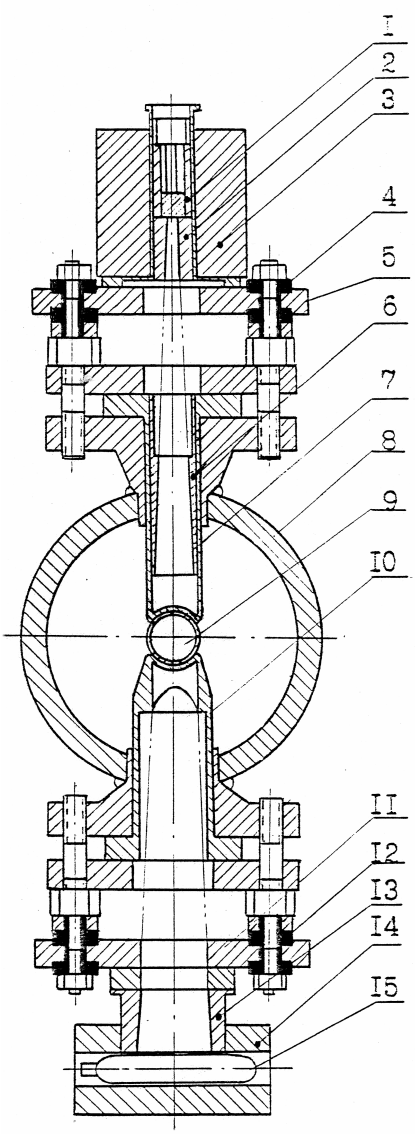

Fig. 3 Gamma-ray device
1 – ampoule with ^{170}Tu;
2, 13 – lead collimators;
3, 14 – cooled containers;
4, 12 – heat-insulating sleeves;
5, 11 – electrical insulation platforms;
6 – steel collimator;
7, 10 – shrouds;
8 –test section;
9 – tested channel (specimen);
15 – gas-discharge counter.

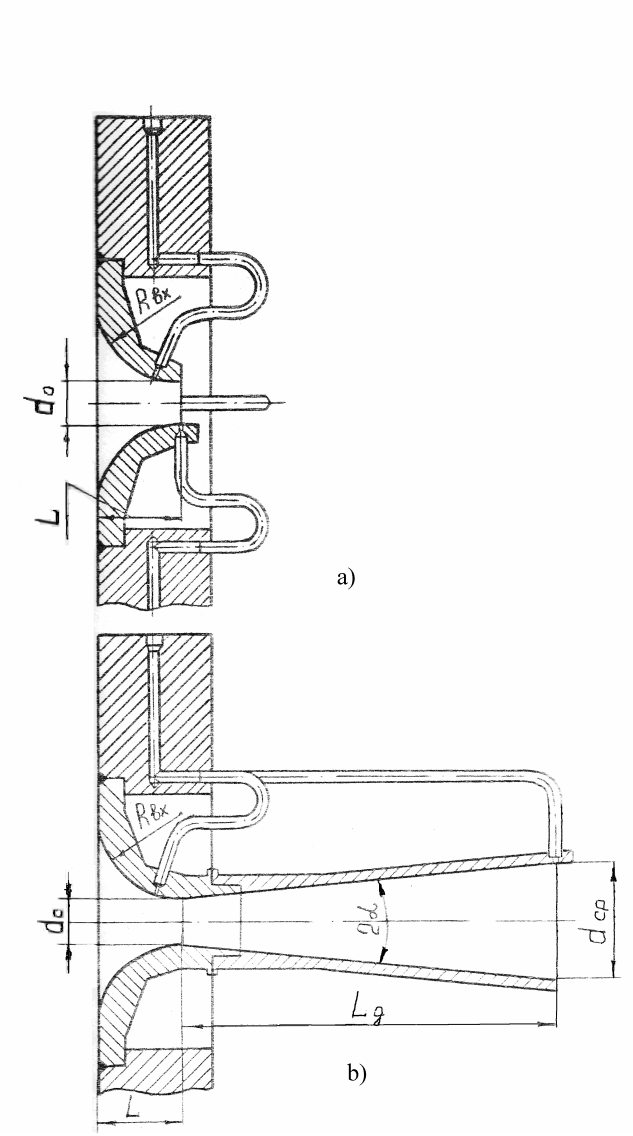

Fig. 4 Converging nozzle (a) and Laval nozzle (b)

2.3 Main measurements

The rates of water and steam flows delivered to the mixer were measured by means of standard nozzles and orifices in pipelines of diameter 50 mm and up. Similar devices in pipelines of smaller diameters were individually calibrated.

Pressure was measured by reference pressure gages (Class 0,1), while the flow temperature was determined by thermocouples with periodic checks for the saturation temperature.

To determine the inlet subcooling, a special manometric device was developed and calibrated, which enhanced considerably the accuracy of measurements.

Steam quality was measured at two sections of six tested channels by exposing the flow to a broad, flat γ-quantum beam.

2.4 Measurement uncertainties

Maximum uncertainties in measurements of thermal-hydraulic parameters were estimated as follows:

- relative uncertainties
  - pressure ± 0.1%
  - mass flow rate ± 3.8%
- absolute uncertainties
  - fluid temperature ± 1.4 °C
  - inlet subcooling ±0.1 °C
  - relative enthalpy x (steam quality)
    for $x < 0.02$ and $x > 1.0$, ± 0.0006
    for $0.02 < x < 1.0$, ± 0.02
  - section-average void fraction, ± 0.05

2.5 Specimens tested

All the tested mockup components of the circulation circuit may be divided into 5 groups of different geometries. The first group included straight and bent tubes with sharp inlet edge. The components within this group differed in their length, diameter and bend location. All in all, there were 26 specimens.

The components of the second group were converging nozzles, Laval nozzles, and Venturi tubes. The 22 specimens of this group differed in the lengths of the cylindrical and diffusion parts as well as in diameters (see Figs. 4 and 5).

The third group consisted of nozzles with a conical inlet, represented by 4 specimens.

The fourth group included tubes with stepped variation of the flow section, z-shaped pipelines, pipeline branches and connections. This group had 9 specimens. One of them is shown in Fig. 6.

The fifth group was represented by the isolation and control valve (ICV) of the RBMK fuel channel with variable opening, tested under direct and reverse flow, Fig. 7.

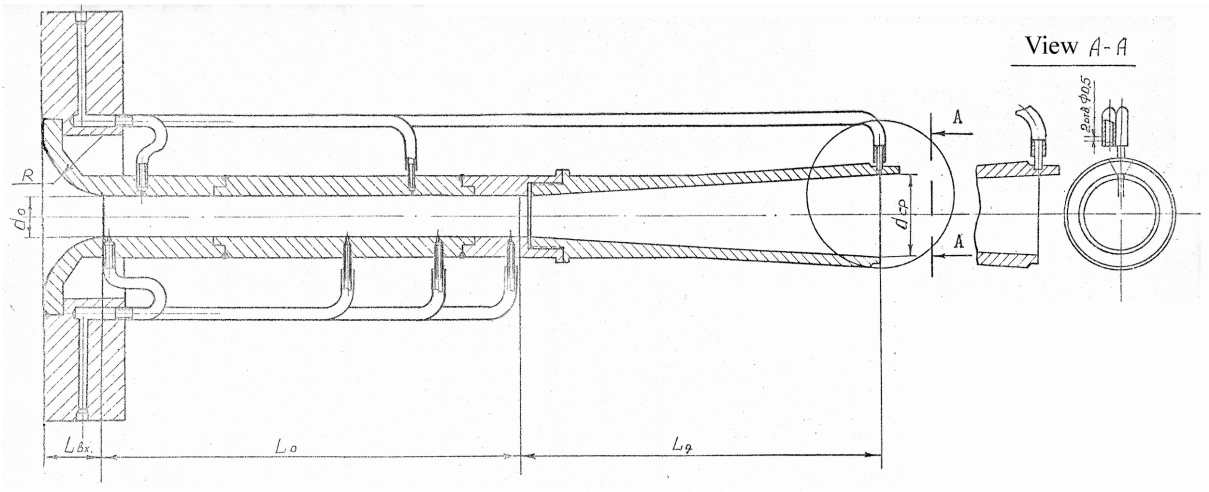

Fig. 5 Venturi tube

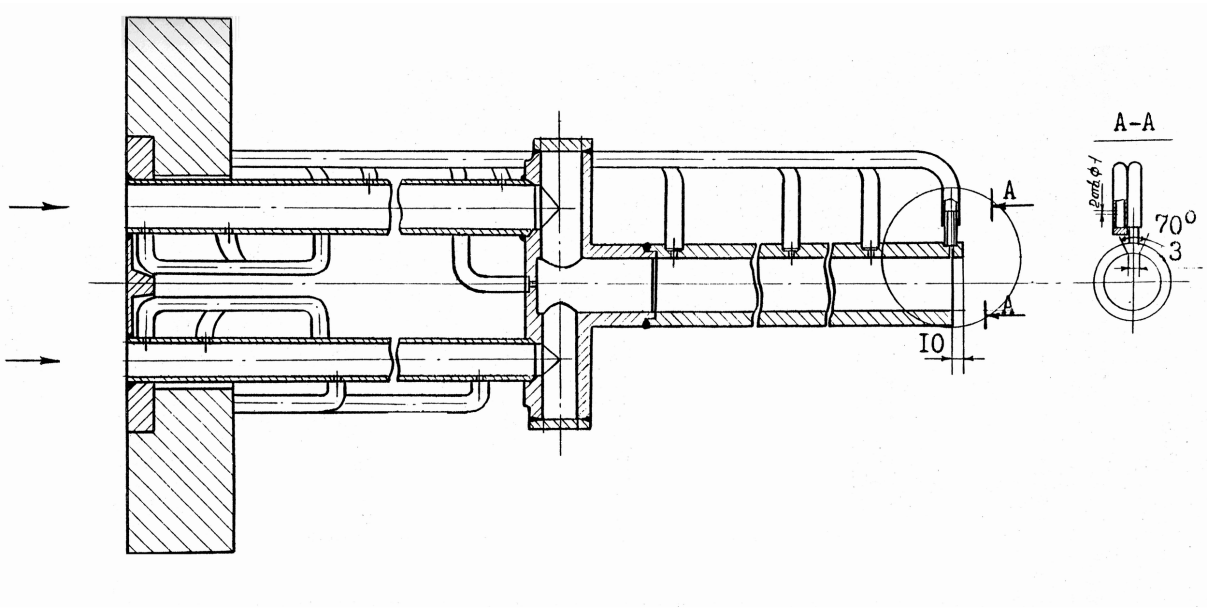

Fig. 6 Connection of two pipelines

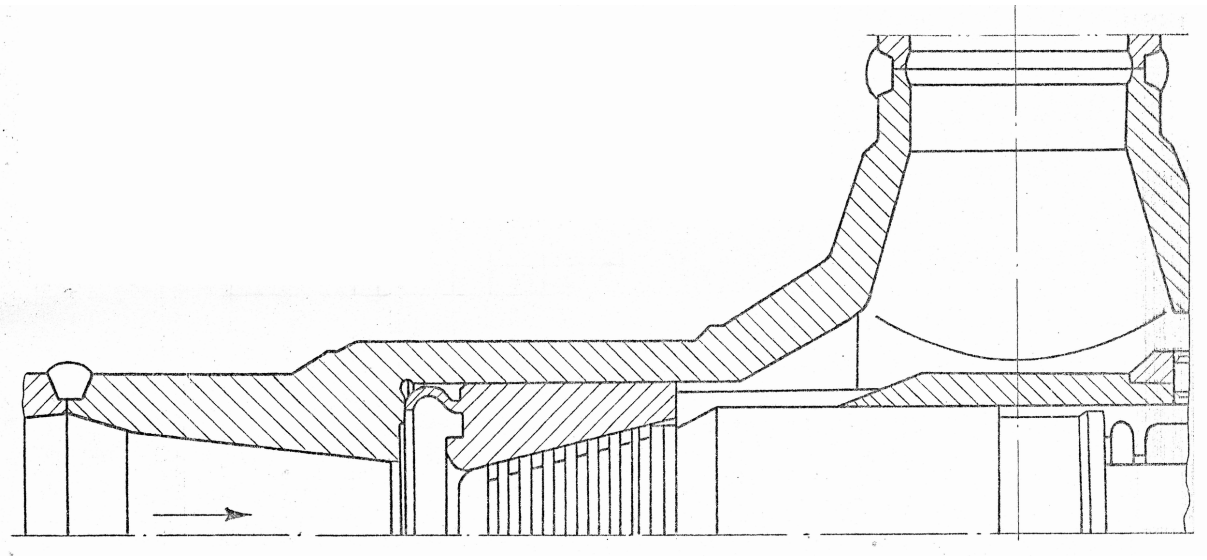

Fig. 7 ICV flow passage. The valve is in the closed position

2.6 Experimental data

All the measurement results are presented in tables, separate for each tested specimen. Table 1 is a fragment of such a table for the tube with a sharp inlet edge, and Table 2 refers to one of the Venturi tube configurations. The data of both tables relate to critical flow conditions. Fig. 8 shows the distribution of static pressure along one of the Venturi tube specimens, with the saturation pressure for each of the experiments indicated in the graph. Subcooled or saturated water was fed to the test section. Local pressure drop below the saturation level near the inlet section led to water flashing and flow choking. Steam and water mixture ran through the tested specimen, accompanied by pressure decrease and growth of void fraction.

Table 1: Tube with a sharp inlet edge

№	P_o	t_o	x_o	ρw	P_1	P_2
40	8.76	295.3	- 0.026	30060	4.77	0.645
41	8.78	299.3	- 0.010	27240	4.50	0.599
42	8.75	301.3	0	25830	4.30	0.572

Static pressure, MPa								Void fraction	
z/d	0.44	2.44	12.02	13.14	27.84	29.84	30.14	30.64	14.0	28.9
40	6.95	7.54	7.39	7.22	6.47	5.83	5.57	2.40	0.140	0.540
41	7.27	7.68	7.34	7.15	6.21	5.58	5.27	2.15	0.330	0.700
42	7.43	7.66	7.17	6.94	5.95	5.29	5.01	2.01	0.500	0.750

Table 2: Venturi tube

№	P_o	t_o	x_o	ρw	Static pressure, MPa; z, mm			
					P_1	P_2	15.4	36.1
56	6.86	267.8	-0.058	47880	1.58	0.542	6.41	5.07
57	6.90	272.1	-0.044	44980	1.50	0.508	6.49	5.31
58	6.87	278.1	-0.023	40770	1.32	0.472	6.54	5.57

In Tables 1 and 2: №– experiment number; P_o – inlet pressure, MPa; t_o – inlet temperature, ^oC; x_o – inlet subcooling (relative enthalpy); ρw – critical mass velocity, kg/(s·m^2); P_1 – pressure at the outlet section of the specimen, MPa; P_2 – pressure downstream of the specimen, MPa; z – distance from the flow inlet, mm;
z/d – relative longitudinal coordinate of the section.

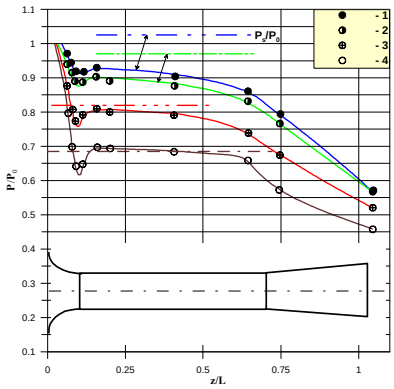

Fig. 8 Pressure distribution along the Venturi tube for P_o = 2.0 MPa with various inlet subcooling, Δt_{so}:
1 – 1.7^{o}C; 2 – 4.3 ^{o}C; 3 – 13.2 ^{o}C; 4 – 21.7 ^{o}C

3. AN EXAMPLE OF EXPERIMENTAL DATA APPLICATION

The 3D-model of single-phase flow in the isolation and control valve (ICV) of the RBMK fuel channel, developed with the use of the 3D hydrodynamic code STAR_CD3.10, was verified against the results of numerous valve tests with different degrees of opening. In the range of operation opening degrees h (from 4 to 12 mm), the values of pressure difference across the valve calculated by the 3D-model departed from the measurements by no more than 4%. In view of the considerable pressure drop in the ICV flow, it was important to determine the conditions under which flashing is possible in the flow part of the valve [Novoselsky, 2007]. To this end, cases with smooth increase of the water flow in the valve to the point of choking were picked out among all the experiments with the fifth group (see Section 2.5). Flow choking pointed to steam generation, to flashing of water in the valve, Fig.9. For this flow condition, calculations were carried out using the 3D-model of the ICV flow passage with analysis of pressure distribution at different flow rates. It was found that, with the water rate identified as a critical flow in that experiment (further pressure decrease downstream of the ICV caused no flow rate growth), a flow zone developed with its pressure below the saturation level, Fig. 10. The zone appeared as a cavitation region, i.e. it was found near a highly curved wall – in the area of transition from toroidal to conical surface of the valve throttle, Fig 11.

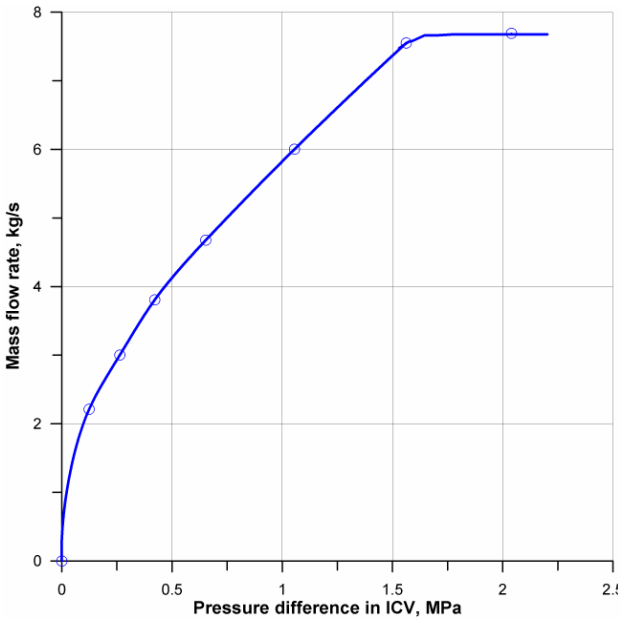

Fig. 9 Flow choking in ICV at P_o = 4.0 MPa, t_o = 170 °C

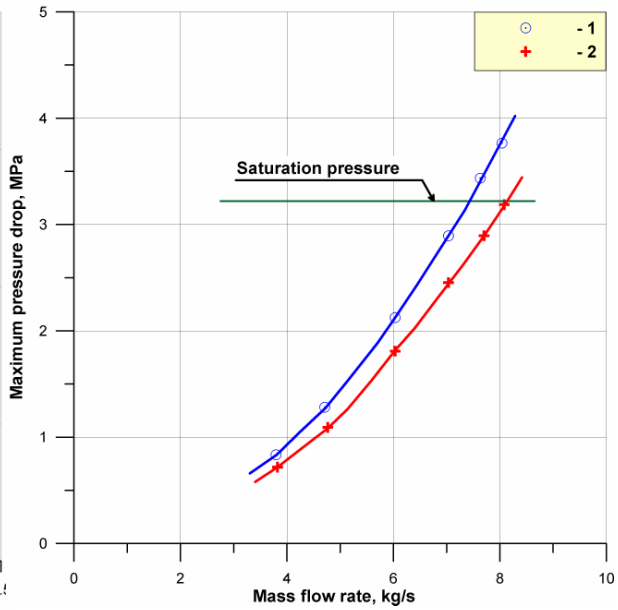

Fig. 10 Maximum pressure drop in ICV (P_o =4.0 MPa, t_o = 170 °C)
1 – at the wall
2 – along the flow passage (section-averaged)

Table 3 contains the results of calculations for the ICV test at the pressure of 4.0 MPa with 5 mm opening. The shadowed column corresponds to flow choking (experiment).

Table 3: Results of calculations for single-phase flow in ICV
h = 5 mm; P_o = 4.0 MPa; t_o = 170 °C; (P_s =0.792 MPa).

Mass flow rate, kg/s	3.78	4.67	6.0	7.0	7.61	7.97
Pressure difference across ICV, MPa	0.39	0.591	0.97	1.32	1.56	1.71
Maximum local pressure drop at the wall, MPa	0.84	1.29	2.13	2.90	3.43	3.76
Maximum pressure drop along the passage, MPa	0.72	1.10	1.82	2.48	2.93	3.23

The zone with pressure below the saturation level is shown in Fig. 11. Fig. 12 illustrates pressure distribution along the flow passage of the ICV throttle. This pressure distribution corresponds to single-phase liquid flow. When in reality steam generation begins at the minimum pressure section, the flow pattern undergoes a considerable change. Increase of volumetric flow rate is accompanied by growth of hydraulic resistance, so instead of rising pressure drops, possibly even below the saturation level. Nevertheless, this process may only be described by a two-phase 3D-model.

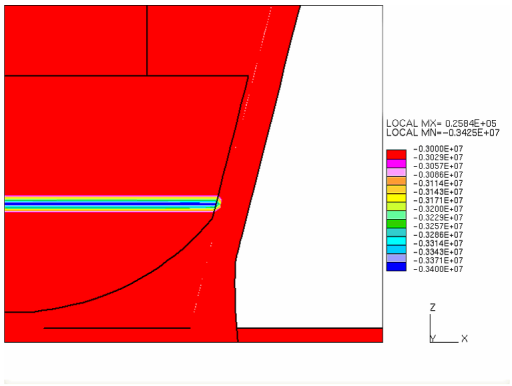

Fig. 11 Local pressure drop at the throttling slit inlet
(ICV opening – 5 mm; inlet pressure – 4.0 MPa; temperature – 170 °C)

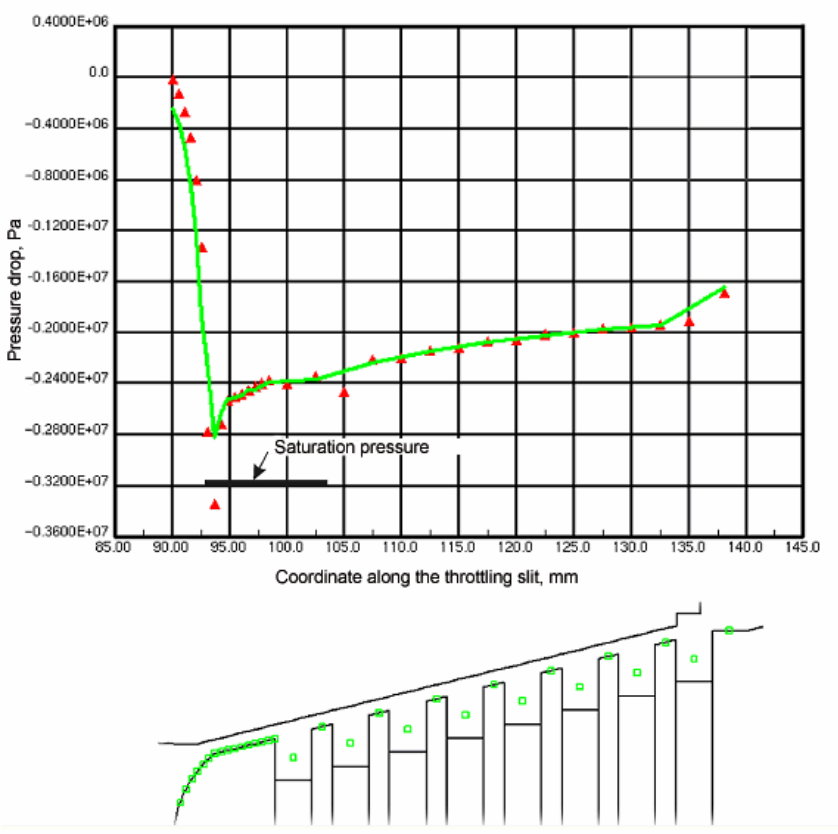

Fig. 12 Pressure distribution along the throttling slit
Triangles – local pressure at the points indicated by squares
in the lower diagram. Conditions – as in Fig. 11

To sum it up, calculations by a 3D-model of single-phase flow and use of experimental data on flow choking in an isolation and control valve made it possible to determine a criterion for steam phase formation and onset of flashing in the ICV flow passage. This criterion is the local pressure decrease at the passage wall by 0.2÷0.5 MPa below the saturation pressure.

References/ Literature

1. U.Graf. P.Papadimitriou. “Simulation of two-phase flow in vertical tubes with the CTFD code FLUBOX”. *Nuclear Engineering and Design* 237 (2007), 2120-2125.
2. R.T.Knapp et al. *Cavitation*, Mc Grow-Hill Book Co, New York, 1970.
3. Novoselsky O.Yu. et al. “Determination of choking appearance in the isolation and control valve using 3D thermal-hydraulic code”. *Teploenergetika*, № 11, 2007, 56-61(in Russian).